JOURNAL OF SOLID STATE CHEMISTRY **103**, 420–432 (1993)

Isothermal Sections and Primary Crystallization in the Quasiternary $YO_{1.5}$–BaO–CuO_x System at $p(O_2) = 0.21 \times 10^5$ Pa

G. KRABBES, W. BIEGER, U. WIESNER, M. RITSCHEL,
AND A. TERESIAK

*Institut für Festkörper- und Werkstofforschung Dresden e.V.,
Helmholtzstr. 20, O-8027 Dresden, Germany*

Received October 17, 1991; in revised form August 26, 1992; accepted September 25, 1992

The phase relations along the sections Y_2BaCuO_5–CuO_x and $YBa_2Cu_3O_{7-\delta}$–CuO_x at temperatures between 900 and 1100°C at 0.21×10^5 Pa O_2 pressure have been investigated by DTA/TG and soaking experiments. Peritectic reaction temperatures have been observed to be 960°C and 940°C, respectively. The results have been combined with literature data to construct a consistent set of isothermal sections in the quasiternary $YO_{1.5}$–BaO–CuO_x system. A precondition of this consideration is the occurrence of only one type of melt which expands over wide ranges of the triangle as the temperature increases. The primary crystallization fields of solid phases have been derived.

1. Introduction

In order to synthesize ceramic samples of high quality and to grow single crystals of $YBa_2Cu_3O_{7-\delta}$ the knowledge of phase relations and phase stabilities as functions of temperature and oxygen partial pressure is of considerable importance. Especially the occurrence of melts is either a restriction or precondition to guarantee optimum manufacturing conditions. Therefore, it should be useful to study melt processing in detail taking into account contradictory literature data.

Most of the papers concerning phase equilibrium investigations are based on DTA/TG measurements along several sections in the $YO_{1.5}$–BaO–CuO_x quasiternary system. Although this consideration is not thoroughly correct because the melting process is combined with an oxygen loss (*1*) it provides a reasonable starting point for understanding the phase relations in the quaternary Y–Ba–Cu–O system. Attempts to systematize these results have been made by Aselage and Keefer (*2, 3*), Holba *et al.* (*4*), Kosmynin *et al.* (*5*), and Osamura and Zhang (*6*), as well as Byeong-Joo Lee and Dong Nyung Lee (*7, 8*). The consideration (*7, 8*) is based on a computer calculation using the concept of free-energy minimization. Taking into account the approachable binary systems and using the published thermodynamic data for the more complicated oxides they obtained a consistent picture of phase diagrams as a parametric function of temperature. One interesting starting point was the supposition of the occurrence of only one type of melt which expands over the whole triangle as the temperature increases.

An additional method which is very useful for phase equilibrium investigations in the presence of a melt is a soaking method pro-

0022-4596/93 \$5.00

posed by Nevriva *et al.* (*9*) to study the primary crystallization field of $YBa_2Cu_3O_{7-\delta}$ from a homogeneous melt. It consists of a separation of the melt from the residual solid by soaking the liquid into a porous substrate.

The present paper contains a comparative study of phase equilibria in the Y–Ba–Cu–O system at 0.21×10^5 Pa O_2 which are obtained by DTA/TG as well as soaking experiments. It aims at a consistent reflection of the melting process in both, a set of isothermal sections in the quasiternary representation $YO_{1.5}$–BaO–CuO_x at temperatures between 900 and 1100°C as well as phase relations along the sections Y_2BaCuO_5–CuO_x and $YBa_2Cu_3O_{7-\delta}$–CuO_x.

2. Experiments

2.1. Synthesis of Initial Compounds

The phases $YBa_2Cu_3O_{7-\delta}$, Y_2BaCuO_5, and $Y_2Cu_2O_5$ which were used in the DTA/TG and soaking experiments have been synthesized in the usual way. Stoichiometric amounts of Y_2O_3 (Merck, p.a.), $BaCO_3$ (P.P.H., Gliwice/Poland, p.a.), and CuO (Ferak, p.a.) were intimately mixed and several times heated at the reaction temperature and ground (123: 2–3 times for 17 h at 900 to 920°C in air, followed by a 24 h annealing at 930°C in O_2; 211: 2 times for 24 h at 930°C in air; $Y_2Cu_2O_5$: 20 h at 960°C in O_2, followed by a 20 h annealing at 985°C in O_2). XRD indicated pure materials. The DTA curve of $YBa_2Cu_3O_{7-\delta}$ showed only one peak at 1020°C and 0.21×10^5 Pa oxygen pressure.

$BaCuO_2$, applied in some investigations, was synthesized as follows. In order to avoid considerable impurities of carbonate the synthesis was started from BaO_2 (Ferak, 99.0%) and CuO. The mixture was primarily heated in argon at 600°C for 5 h to avoid the melting of BaO_2. After repeated 24 h annealing at 900°C and 950°C, respectively, in O_2 and grinding, the XRD pure material had a carbon content of less than 0.1 mass%.

Starting from $BaCuO_2$ and Cu, $BaCu_2O_2$ was synthesized by a 2 day annealing at 850°C in argon, followed by a quenching in liquid N_2.

2.2. Thermal Analysis

DTA/TG investigations have been carried out with a heating rate of 10 K/min from room temperature to 1100°C using a Setaram TG/DTA 92 apparatus. The oxygen partial pressure of 0.21×10^5 Pa in the flowing oxygen–argon mixture was controlled by a zirconia-e.m.f. cell.

2.3. Soaking Method

In addition to thermal analysis the soaking method (*9*) is a reasonable tool to further clarify the phase relations in the presence of a melt. A pellet of a homogeneous mixture of defined composition the melting behavior of which is to be investigated is placed on a porous substrate tablet. In order to guarantee a solid state prereaction of the initial compounds, sample and substrate were heated at a temperature about 20 K below the expected (partial) melting temperature for 3 hr. Then the temperature was quickly raised to the equilibration temperature T, held at T for 24 to 48 hr, and quenched. The temperature measurement is calibrated by the melting point of silver (960°C) imbedded in a 123 tablet. Supposing that no metastable melts or phases are formed before the equilibrium is established, the arising melt is soaked by the substrate tablet. This soaking must provide an almost quantitative separation of melt and coexisting solid phase(s). On the other hand, the substrate has to be chemically inert. Therefore, such a substrate phase was chosen which coexists with the initial mixture below T as well as the solid reaction products and the arising melt at T. Y_2O_3 is an appropriate substrate for the investigation of melting equilibria along the section

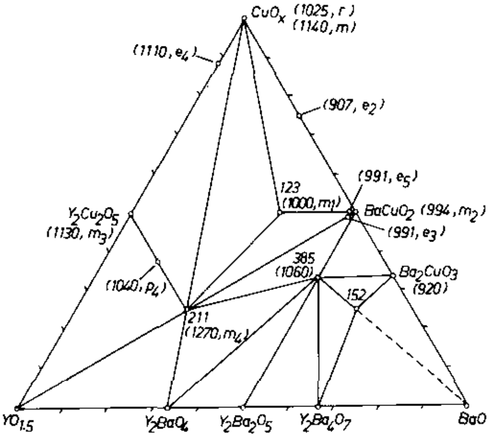

FIG. 1. Quasiternary phase diagram $YO_{1.5}$–BaO–CuO at 875°C and favored temperatures of first melt occurrence: (e) eutectics; (p) peritectics; (m) congruent melting; (r) reduction.

Y_2BaCuO_5–CuO_x and Y_2BaCuO_5 was applied for $YBa_2Cu_3O_{7-\delta}$–CuO_x mixtures (compare Fig. 1). This choice also guarantees the absence of ternary eutectics within the triangles substrate–initial mixture.

The residual solid is characterized by XRD and wet chemical analysis. Owing to the adhesion of remaining parts of the melt in the residual tablet the results of the chemical analysis are only roughly a measure for quantitative melt composition. Therefore, the melt compositions of the invariant reactions p_1, p_2, and p_4 (compare Section 3.5) have been approximately derived by the geometric join of the extrapolated tie lines of reaction products and initial mixture compositions determined from the soaking experiments along the sections $YBa_2Cu_3O_{7-\delta}$–CuO_x, Y_2BaCuO_5–CuO_x, and $Y_2Cu_2O_5$–Y_2BaCuO_5, respectively.

3. Results and Discussion

3.1. Melting and Decomposition Behavior of Pure Phases and Binary Mixtures

In order to construct a consistent picture the following literature data and experimental results have been taken into consideration.

$YBa_2Cu_3O_{7-\delta}$. The 123 phase is reported to decompose peritectically into Y_2BaCuO_5 and a melt. The corresponding temperature differs between 980°C (see, e.g., (*10*)) and 1015°C (see, e.g., (*2*, *11*)). According to Osamura and Zhang the peritectic decomposition of 123 at 1010°C leads to the formation of a 143 phase besides 211 and melt (*6*). Soaking experiments carried out in our laboratory confirm the peritectic decomposition into 211 and melt at 1000°C $< T <$ 1010°C. As discussed in Section 2.1, DTA at 0.21×10^5 Pa O_2 indicated a reaction at 1020°C which is accepted for further discussion. No 143 phase was found.

Y_2BaCuO_5. At considerably higher temperatures (≈1270°C), Y_2BaCuO_5 will be peritectically decomposed into Y_2O_3 and a copper and barium rich melt (see, e.g., (*2*, *11*)). The copper valency +2 should remain unchanged up to the decomposition point despite a variable metal ratio at high temperatures.

CuO/Cu_2O. CuO will be reduced in air at 1025°C to Cu_2O, which melts at 1140°C under increasing oxygen content of the melt (see, e.g., (*12*)).

$BaCuO_2$. The decomposition behavior of $BaCuO_2$ has not been clarified in detail until now. Whereas Grebenshchikov and coworkers (*13*) discussed a peritectic decomposition, Zhang *et al.* (*14*) proposed a monotectic melting at 1016°C. Aselage and Keefer (*2*) found a congruent melting at 1014°C. According to soaking experiments, $BaCuO_2$ melts congruently in view to the metal content at about 1005°C (*15*); however, monotectic melting behavior cannot be excluded by this method. Because the DTA study of $BaCuO_2$ at 0.21×10^5 Pa O_2 indicated only one single endothermic signal at 994°C, a congruent melting of $BaCuO_2$ is assumed in the following consideration.

A Ba rich Ba_2CuO_3 phase is reported by Zhang *et al.* (*14*) to melt incongruently at

920°C. The Cu rich $Ba_2Cu_3O_{5+x}$ phase discussed by Thompson *et al.* (*16*) should not be stable in air in the considered temperature region. The existence of $BaCu_2O_2$ (*17*) at 0.21×10^5 Pa (predicted, e.g., in (*4*)) could not be confirmed by our own experiments in the considered temperature region.

$Y_2Cu_2O_5$. Most authors observed a peritectic decomposition of $Y_2Cu_2O_5$ to Y_2O_3 and a melt at about 1130°C (see, e.g., (*2, 18*)). The reduced compound $YCuO_2$ discussed at lower oxygen pressures (see, e.g., (*19*)) is expected not to be stable in air, as is concluded from the thermodynamic data evaluated in (*19*) and the investigations by Zhang and Osamura (*20*). But its occurrence sensitively depends on the real oxygen pressure because the peritectic decomposition temperature of $Y_2Cu_2O_5$ at $p(O_2) = 0.21 \times 10^5$ Pa is very close to the reduction temperature (*21*). Experiments performed in our laboratory confirm this sensitive behavior: Whereas the TG measurements of pure $Y_2Cu_2O_5$ at 0.21×10^5 Pa O_2 did not give rise to an intermediate formation of $YCuO_2$, DTA/TG investigations at 0.13×10^5 Pa O_2 clearly indicate two distinct signals are caused by the formation of $YCuO_2$ followed by its peritectic decomposition.

$Y_3Ba_8O_5O_z$. Only a few authors focused their interest on the decomposition behavior of the 385 phase. The 385 stoichiometry should be a better reflection of the structure than 132 or 143. Probably this phase is a solid solution. According to Klinkova *et al.* (*22*) the phase should be stable up to 1060°C.

$BaCuO_2$–CuO. The eutectic temperature along this section discussed by several authors varied between 890°C (*14*) and 920°C (*2*). According to our DTA/TG investigations the eutectic mixture at 75 mol% CuO/25 mol% BaO melts at 907°C. Melting is accompanied by a considerable oxygen loss (*1, 15*).

$Y_2Cu_2O_5$–CuO_x. Whereas Nevriva *et al.* (*23*) as well as Zhang and Osamura (*20*) found a eutectic temperature at 1075°C, Aselage and Keefer (*2*) published a value of 1110°C. A theoretical calculation led to a eutectic temperature of 1030°C (*24*). The eutectic composition is about 22 mol% $Y_2Cu_2O_5$ (*2*). As it will be clear in the discussion below we favor the higher temperature.

$BaCuO_2$–$YBa_2Cu_3O_{7-\delta}$. Different opinions concerning the melting mechanism along this section have been published. Whereas Mesenzeva *et al.* (*25*) (850°C), Grebenshchikov *et al.* (*26*) (910°C), and Fotiev *et al.* (*27*) (1005°C) discussed eutectic behavior, Aselage and Keefer (*2*) favored a peritectic process into 211 + L and Nevriva *et al.* (*28*) supposed a decomposition into solid phases. DTA/TG measurements of 123 + $BaCuO_2$ mixtures of various compositions indicated three endothermal signals over wide ranges of the section. Independent of the initial composition the first peak was found at 991°C and the second one at about 1010°C for $x(BaCuO_2) < 80$ mol% (Σ metals = 1). Therefore, just below the temperature where the 123 phase is peritectically decomposed and $BaCuO_2$ is melting, a reaction including both compounds leads to the formation of a melt (denoted as e_5) the composition of which is located near the $BaCuO_2$ phase (>95 mol% $BaCuO_2$).

$BaCuO_2$–Y_2BaCuO_5. A eutectic point at about 1000°C with a composition near the $BaCuO_2$ phase has been found by several authors (e.g., (*2, 13, 27*)). On the other hand, Osamura and Zhang (*6*) as well as Roth *et al.* (*18*) refer to a qualitative change of phase relations at about 910°C: The solid state reaction 211 + $BaCuO_2$ should lead to the formation of 123 and a Ba rich phase (143 in CO_2-free air, 184 in natural air). Experiments performed in our laboratory show that the $BaCuO_2$–Y_2BaCuO_5 coexistence will be stable at least up to 950°C. An initial mixture of 123 and 385 is partly transformed into 211 and $BaCuO_2$ by 3 days annealing at 950°C, whereas mixtures of 211 and $BaCuO_2$ remain unchanged under the same conditions.

DTA/TG measurements of $BaCuO_2$+ 211 mixtures indicated a first peak at 991°C which coincides with that of reaction e_5. A detailed discussion of the changes of phase relations in this region including the oxygen stoichiometry change will be given elsewhere (*29*).

$Y_2Cu_2O_5$–Y_2BaCuO_5. Mikirticheva *et al.* (*13*) observed the appearance of a melt along this section at 1080°C. Soaking experiments performed in our laboratory indicate that the considered coexistence is already disconnected at 1040°C by the formation of the Y_2O_3 + L two phase region.

The sections $YBa_2Cu_3O_{7-\delta}$–CuO_x and Y_2BaCuO_5–CuO_x will be discussed in detail below.

In order to determine the lowest melting point of the quasiternary system (e_1 in the notation of (*2*)) several authors investigated the phase relations within the quasiternary $BaCuO_2$–$YBa_2Cu_3O_{7-\delta}$–CuO_x phase field (e.g., (*2, 21, 30–32*)). DTA measurements performed in our laboratory within the considered triangle verify a temperature of 899°C at $p(O_2) = 0.21 \times 10^5$ Pa which confirms the value in (*2*). From the evaluation of DTA heat flow its composition has been determined to be close to (1.25 mol% $YO_{1.5}$, 28.75 mol% BaO, 70 mol% CuO).

A quasiternary phase diagram $YO_{1.5}$–BaO–CuO at about 875°C is shown in Fig. 1, where the favored values for the first occurrence of a melt for pure phases and binary mixtures have been included. The phase relations in the barium rich part of the diagram have been taken from (*33*).

3.2. The Polythermal Section $YBa_2Cu_3O_{7-\delta}$–CuO_x

Partial melting of mixtures of $YBa_2Cu_3O_{7-\delta}$ and CuO has been observed by several authors at about 940°C (e.g., (*2, 11*)) but the whole melting process seems to be very complicated. A first attempt to explain possible phase equilibria at higher temperatures using DTA/TG measurements in air and O_2 has been published by Licci *et al.* (*34*). Additional experimental information using a complementary method is useful to further clarify the considered diagram.

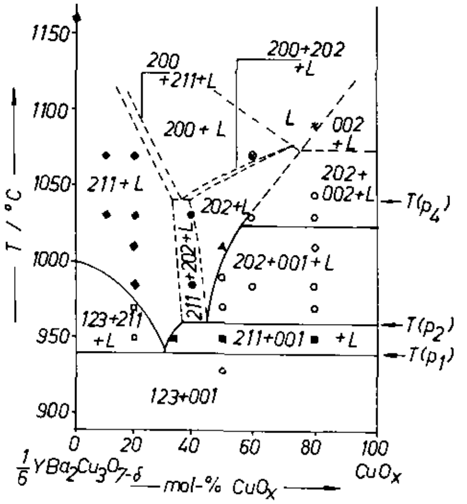

FIG. 2. Soaking experiments along the section $\frac{1}{6}$ $YBa_2Cu_3O_{7-\delta}$–CuO_x and deduced possible phase equilibria: (◇) 123 + CuO, (□) 123 + 211 + L, (■) CuO + 211 + L, (◆) 211 + L, (●) $Y_2Cu_2O_5$ + 211 + L, (▲) $Y_2Cu_2O_5$ + L, (○) $Y_2Cu_2O_5$ + CuO_x + L, (▼) Y_2O_3 + 211 + L, (⊗) Y_2O_3 + L, (*) L, (123) $YBa_2Cu_3O_{7-\delta}$, (001) CuO, (211) Y_2BaCuO_5, (202) $Y_2Cu_2O_5$, (200) Y_2O_3, (002) Cu_2O, (L) melt.

In the present paper the phase equilibria along the 123–CuO_x section have been investigated by soaking experiments of several mixtures at temperatures between 920°C and 1080°C, see Fig. 2. Y_2BaCuO_5 is chosen as substrate phase because it coexists with both $YBa_2Cu_3O_{7-\delta}$ and CuO_x below 920°C. Furthermore, Y_2BaCuO_5 is expected to form an equilibrium with the melt. The results are collected in Table I. The XRD analysis of one single 1 : 1 mixture indicated the coexistence of both phases at 930°C. By raising the temperature to 950°C a part of the initial mass has been melted and soaked by the substrate. The coexistence between 123 and CuO is displaced by two three phase

TABLE I

SOAKING EXPERIMENTS ALONG THE SECTION $YBa_2Cu_3O_{7-\delta}$–CuO_x

No.	Temp. (°C)	Initial mixture (mol%)		Mass loss (%)	XRD of residual solids	
		123	CuO_x		Main phases	Secondary phases
1	930	50	50	1.2	123 + CuO	
2	950	80	20	56.5	211 + 123	
3	950	50	50	53.3	211 + CuO	$Y_2Cu_2O_5$
4	950	20	80	21.0	CuO + 211	
5	970	80	20	67.5	211 + 123	
6	970	50	50	80.5	$Y_2Cu_2O_5$ + CuO	
7	970	20	80	37.4	CuO + $Y_2Cu_2O_5$	
8	985	80	20	71.7	211	
9	985	60	40	79.8	211 + $Y_2Cu_2O_5$	
10	985	40	60	74.2	CuO + $Y_2Cu_2O_5$	
11	985	20	80	39.0	CuO + $Y_2Cu_2O_5$	
12	990	100	0	5.6	123	
13	990	50	50	83.1	$Y_2Cu_2O_5$ + CuO	
14	1010	100	0	59.6	211	(Ba_3CuO_4)
15	1010	80	20	72.4	211	$Y_2Cu_2O_5$
16	1010	50	50	84.5	$Y_2Cu_2O_5$	
17	1010	20	80	46.4	CuO + $Y_2Cu_2O_5$	
18	1030	90	10	55.4	211	(CuO)
19	1030	80	20	67.0	211	
20	1030	60	40	76.9	211 + $Y_2Cu_2O_5$	Y_2O_3 + $BaCuO_2$
21	1030	40	60	81.2	$Y_2Cu_2O_5$ + CuO	
22	1030	20	80	68.0	CuO + $Y_2Cu_2O_5$	
23	1045	20	80	93.5	$Y_2Cu_2O_5$ + CuO + (Y_2O_3)	
24	1070	90	10	66.8	211	$BaCuO_2$
25	1070	80	20	60.5	211	$BaCuO_2$ + (CuO)
26	1070	40	60	92.8	Y_2O_3	(CuO)
27	1070	20	80	95.9	($Y_2Cu_2O_5$)	
28	1090	20	80	100.0	—	—
29	1160	100	0	61.6	211	($BaCuO_2$)

equilibria, 211 + 123 + L and 211 + CuO + L, respectively, separated by the two phase region 211 + L. The isothermal section $YO_{1.5}$–BaO–CuO is changing at about 940°C as is shown in Fig. 3a. The observed temperature is in good agreement with the value dynamically obtained by other authors (*2*, *11*). Already at 970°C, XRD of the residue of CuO rich mixtures indicated $Y_2Cu_2O_5$ besides CuO. This means that $Y_2Cu_2O_5$ forms a further equilibrium with the liquid at about 960°C. As shown in Fig. 3b, the 211 + CuO equilibrium will be intersected by the coexistence of $Y_2Cu_2O_5$ + L, forming two new three phase equilibria, $Y_2Cu_2O_5$ + CuO + L and 211 + $Y_2Cu_2O_5$ + L.

The characteristic changes of phase relations at the e_5 reaction 123 + $BaCuO_2$ → 143 + L (991°C) and the peritectic decomposition temperature of 123 (1020°C) are shown in Figs. 3c and 3d, respectively. At nearly the same temperature (994°C) $BaCuO_2$ melts congruently with respect to the metal ratio.

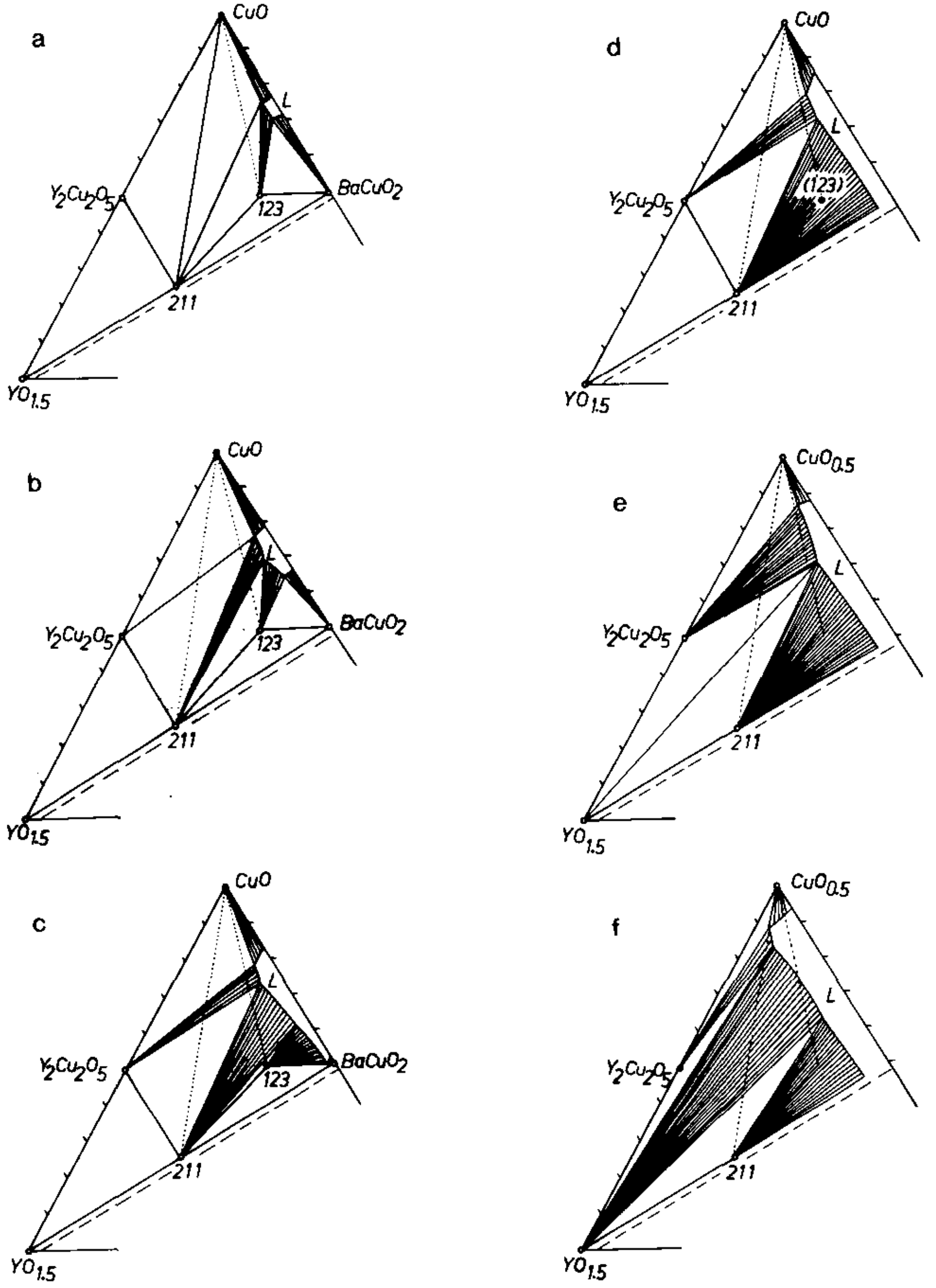

FIG. 3. Three dimensional projections $YO_{1.5}$–BaO–CuO_x of isothermal sections at (a) 940°C, (b) 960°C, (c) 991°C, (d) 1020°C, (e) 1040°C, and (f) ≈1090°C. (The dotted lines correspond to the sections considered in Figs. 2 and 4.)

Soaking experiments at 985°C and 1010°C indicate that the $Y_2Cu_2O_5$ + L equilibrium range becomes broader but the phase relations do not change on principle. Above 1040°C, Y_2O_3 is identified as part of the residual solid indicating the formation of the Y_2O_3 + 211 + L and Y_2O_3 + $Y_2Cu_2O_5$ + L three phase fields (Fig. 3e). This observation contradicts the opinion of Aselage *et al.* (*3*) who discussed a region of homogeneous melt along this section already at about 970°C. According to soaking experiments, complete melting was observed only above 1070°C with an initial CuO_x content of about 80 mol%.

3.3. *The Polythermal Section Y_2BaCuO_5–CuO_x*

Partial melting along the 211–CuO_x section has been reported to start at 970°C (*25*) and 987°C (*2*), respectively. DTA investigations carried out in our laboratory confirm these results. An endothermal peak was observed at 968°C. This temperature corresponds to the value obtained by soaking along the 123–CuO_x section as discussed in the previous section. According to this study the formation of the $Y_2Cu_2O_5$ + L equilibrium at 960°C leads also to the intersection of the 211–CuO coexistence, see Figs. 4 and 3b.

Up to about 1030°C soaking experiments as well as the absence of DTA signals verify that the phase equilibria along the considered section do not change in this temperature region. Small amounts of CuO besides a majority of $Y_2Cu_2O_5$ (XRD of experiments 5 and 6 in Table II) are interpreted as being caused by the crystallization of the residual melt. This should be current also for other experiments where secondary phases have been detected. Above 1025°C Cu_2O joins the diagram instead of CuO at 0.21 × 10^5 Pa O_2.

The residue of soaking experiments at 1040°C contains Y_2O_3 in addition to 211 and/or $Y_2Cu_2O_5$ in the Y_2BaCuO_5 rich part of the section. The change of the isothermal representation by forming the Y_2O_3 + L equilibrium is shown in Fig. 3e. Consequently, the new three phase equilibria, 211 + Y_2O_3 + L and Y_2O_3 + $Y_2Cu_2O_5$ + L, arise. This result confirms the soaking experiments along the section $Y_2Cu_2O_5$–211 and excludes a coexistence of $Y_2Cu_2O_5$ and 211 up to 1080°C as it was discussed in (*13*) (see Section 3.1). DTA/TG measurements along the 211–CuO_x section indicated changes in equilibrium phase composition at 1055°C. Because the corresponding peaks of the cooling process have been observed at 1020°C the phase conversion may be controlled by kinetics and the real temperature should be between both values.

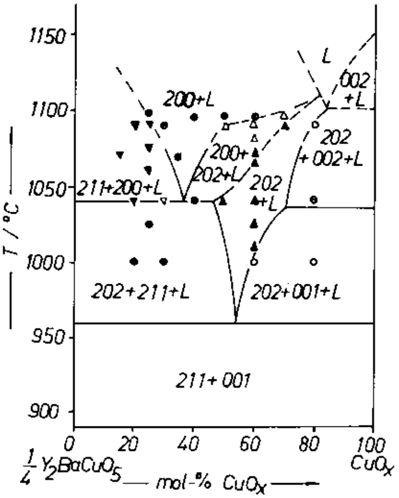

FIG. 4. Soaking experiments along the section $\frac{1}{4}$ Y_2BaCuO_5–CuO_x and deduced possible phase equilibria. For symbols see Fig. 2, (△) Y_2O_3 + $Y_2Cu_2O_5$ + L, (▽) Y_2O_3 + $Y_2Cu_2O_5$ + 211 + L, (⊖) $Y_2Cu_2O_5$ + CuO + Cu_2O + L.

A proposal of possible changes at higher temperatures is marked by broken lines in Fig. 4. The soaking experiments carried out at 1090°C did not give any indication of a single phase homogeneous melt. On the other hand, the binary eutectic temperature $Y_2Cu_2O_5$–Cu_2O is reported to be at about

TABLE II

SOAKING EXPERIMENTS ALONG THE SECTION Y_2BaCuO_5–CuO_x

		Initial mixture (mol%)			XRD of residual solids	
No.	Temp. (°C)	CuO_x	211	Mass loss (%)	Main phases	Secondary phases
1	1000	80	20	33.6	$Y_2Cu_2O_5$ + CuO	
2	1000	60	40	56.8	$Y_2Cu_2O_5$ + CuO	
3	1000	30	70	22.2	$Y_2Cu_2O_5$ + 211	
4	1000	20	80	17.7	$Y_2Cu_2O_5$ + 211	
5	1010	60	40	58.6	$Y_2Cu_2O_5$	CuO
6	1025	60	40	58.7	$Y_2Cu_2O_5$	CuO
7	1025	25	75	24.2	211 + $Y_2Cu_2O_5$	
8	1040	80	20	53.9	$Y_2Cu_2O_5$ + Cu_2O + CuO	
9	1040	60	40	56.8	$Y_2Cu_2O_5$	
10	1040	50	50		$Y_2Cu_2O_5$	Y_2O_3
11	1040	40	60	50.3	$Y_2Cu_2O_5$ + 211, (Y_2O_3)	
12	1040	30	70	47.0	Y_2O_3 + $Y_2Cu_2O_5$ + 211	123
13	1040	20	80	25.9	211 + Y_2O_3	123
14	1060	25	75	50.4	Y_2O_3 + 211	$Y_2Cu_2O_5$
15	1065	60	40	59.7	$Y_2Cu_2O_5$	
16	1070	15	85	36.5	Y_2O_3 + 211	
17	1070	35	65	62.3	Y_2O_3	
18	1072	60	40	59.3	$Y_2Cu_2O_5$ + Y_2O_3	
19	1075	25	75	46.8	Y_2O_3 + 211	
20	1080	60	40	60.2	$Y_2Cu_2O_5$ + Y_2O_3	
21	1090	80	20	78.8	$Y_2Cu_2O_5$ + Cu_2O	
22	1090	70	30	71.5	$Y_2Cu_2O_5$	
23	1090	60	40	64.7	$Y_2Cu_2O_5$ + Y_2O_3	
24	1090	50	50		Y_2O_3 + $Y_2Cu_2O_5$	
25	1090	30	70	57.6	Y_2O_3	$Y_2Cu_2O_5$, 123
26	1090	25	75	48.3	Y_2O_3 + 211	$Y_2Cu_2O_5$
27	1090	20	80	36.6	211 + Y_2O_3	123
28	1095	70	30	71.0	$Y_2Cu_2O_5$ + Y_2O_3	
29	1095	60	40	75.0	Y_2O_3	
30	1095	50	50	68.9	Y_2O_3	$Y_2Cu_2O_5$
31	1095	40	60		Y_2O_3	$Y_2Cu_2O_5$
32	1100	25	75	49.7	Y_2O_3	211

1110°C (*2*). Therefore, the temperature where the region of homogeneous melt joins the considered section is extrapolated to be about 1090°C (Fig. 3f). The phase fields $Y_2Cu_2O_5$ + L and $Y_2Cu_2O_5$ + Y_2O_3 + L are limited by the peritectic decomposition of $Y_2Cu_2O_5$ at 1130°C (*2*) (compare Section 3.1). A temperature of 1100°C is accepted as a probable value where the $Y_2Cu_2O_5$ phase disappears along the 211–CuO_x line.

3.4. Liquidus Surface Considerations

The primary crystallization fields of solid phases from the homogeneous melt have been derived on the base of the isothermal sections (Fig. 3). The approximative melt compositions (in mol%) and temperatures corresponding to the reactions (in the notation of Aselage and Keefer (*2*, *3*))

---

p_1: $YBa_2Cu_3O_{7-\delta} + CuO \rightarrow Y_2BaCuO_5 + L$ (940°C, Soaking)

p_2: $Y_2BaCuO_5 + CuO \rightarrow Y_2Cu_2O_5 + L$ (960°C, Soaking)

p_4: $Y_2BaCuO_5 + Y_2Cu_2O_5 \rightarrow Y_2O_3 + L$ (1040°C, Soaking)

m_1: $YBa_2Cu_3O_{7-\delta} \rightarrow Y_2BaCuO_5 + L$ (1020°C, DTA)

e_1: $YBa_2Cu_3O_{7-\delta} + BaCuO_2 + CuO \rightarrow L$ (899°C, DTA)

e_5: $YBa_2Cu_3O_{7-\delta} + BaCuO_2 \rightarrow L + 143$ (991°C, DTA)

---

have been determined from Fig. 3:

p_1: (YO$_{1.5}$: 3.7, BaO: 22.3, CuO: 74.0);

p_2: (4.0, 20.0, 76.0); p_4: (7.5, 22.0, 70.5);

m_1: (4.0, 36.5, 59.5); e_1: (1.25, 31.25, 67.5);

e_5: (0.4, 49.2, 50.4).

It is worth noting that in contrast to the primary crystallization field proposed by Aselage and Keefer (*2*), the p_2 and p_4 compositions are located in the $YBa_2Cu_3O_{7-\delta}$–$BaCuO_2$–CuO triangle. This results from the soaking experiments along the $YBa_2Cu_3O_{7-\delta}$–CuO_x section which, in the case of suitable initial mixtures, indicate both $Y_2Cu_2O_5$ and/or Y_2O_3 in the residual solid.

The liquidus surface derived from these invariant reactions is shown in Fig. 5. The primary crystallization field for the $YBa_2Cu_3O_{7-\delta}$ phase is rather limited. It stretches from about 1 to 6 mol% YO$_{1.5}$ and about 50 to 74 mol% CuO. The considered region is adjoined by the CuO, 211, and $BaCuO_2$ crystallization fields.

In order to prove the deduction of the $YBa_2Cu_3O_{7-\delta}$ crystallization field, the following experiments have been carried out:

Mixtures of $YBa_2Cu_3O_{7-\delta}$, $BaCuO_2$, and CuO, the composition of which is chosen to be within or near the 123 primary crystallization field, have been soaked on Y_2BaCuO_5 about 10 K below the temperature where a homogeneous melting of the entire mixture is expected. The small amount of residual solid was characterized by XRD (Table III). Mostly, the phase left in the sample was pure $YBa_2Cu_3O_{7-\delta}$, indicating that this phase can probably be considered to be stable just below the liquidus surface at the chosen initial composition.

Furthermore, the p_1–m_1 boundary of the primary crystallization field was confirmed by crystal growth experiments with $YBa_2Cu_3O_{7-\delta}$ carried out in our laboratory, quite in agreement with Ref. (*35*). The e_1–e_5 boundary is estimated on the base of these experiments and is approximately represented by a straight line.

3.5. Oxygen Content of the Melt

TG investigations of the invariant reactions derived in Section 3.4 using a Perkin–Elmer TGA 7 thermobalance indicate a sudden mass change at the conversion temperatures. Taking into account the corresponding approximative melt compositions, a formal CuO$_x$ stoichiometry of the melt can be calculated. Independent of the reaction temperature, an x value of 0.68 ± 0.03 has been determined (*29*). Therefore, the melt composition corresponds to a YO$_{1.5}$–BaO–CuO"$_{0.68}$" section, a preferable

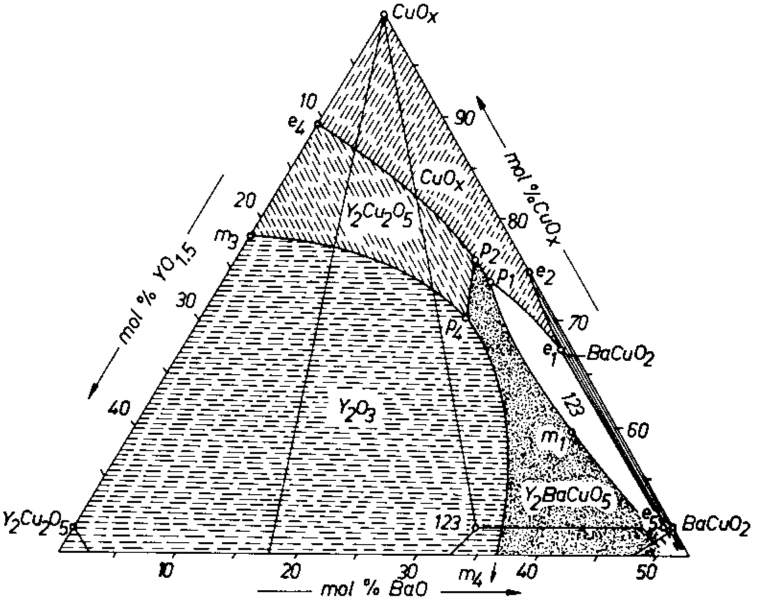

FIG. 5. Primary crystallization fields of solid phases in the $YO_{1.5}$–BaO–CuO_x system derived from the isothermal sections in Fig. 3. (m_1, p_1, p_2, p_4, e_1, e_5) This work; (e_2) taken from (*1*, *15*); (e_4, m_3, m_4) taken from (*2*). (The e_1 composition is redetermined in (29), see text.)

TABLE III

SOAKING EXPERIMENTS WITHIN OR NEAR THE DEDUCED PRIMARY CRYSTALLIZATION FIELD OF $YBa_2Cu_3O_{7-\delta}$

No.	Temp. (°C)	Composition[a]			Mass loss (%)	XRD of residual solids	
		$YO_{1.5}$	BaO	CuO		Main phases	Impurities
1	950	5	22.5	72.5	53.9	123 + CuO	
2	950	3.75	23.75	72.5	85.9	123	211
3	950	2.5	25	72.5	62.9	123	211
4	960	5	25	70	79.1	123	211
5	960	3.75	26.25	70	79.2	123	
6	960	2.5	27.5	70	81.4	123 + $BaCuO_2$	
7	970	5	27.5	67.5	51.1	123	
8	970	3.75	28.75	67.5	77.6	123	
9	970	2.5	30	67.5	74.9	123 + $BaCuO_2$	
10	980	5	30	65	80.5	123	211
11	980	3.75	31.25	65	92.1	211	123
12	980	2.5	32.5	65	74.5	123 + $BaCuO_2$	
13	990	5	32.5	62.5	89.8	211	
14	990	3.75	33.75	62.5	82.1	123	211

[a] Point (in mol%) within the quasiternary representation $YO_{1.5}$–BaO–CuO. However, the initial mixture was formed from $YBa_2Cu_3O_{7-\delta}$, $BaCuO_2$, and CuO.

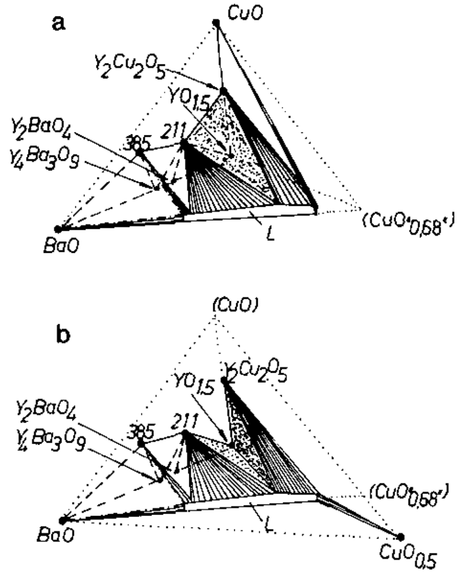

FIG. 6. $YO_{1.5}$–BaO–$CuO_{0.5}$–CuO quasiquaternary representation of the change of phase relations from 1020 to 1040°C: (a) $T \approx 1020°C$; (b) $T \approx 1040°C$.

plane within the $YO_{1.5}$–BaO–CuO–$CuO_{0.5}$ quasiquaternary system and, consequently, in the presence of a melt, the Y–Ba–Cu–O system has to be considered as a real quaternary one.

This is exemplarily demonstrated in Fig. 6 for the significant change of phase relations at the p_4 invariant reaction temperature (1040°C). The coexistence between $Y_2Cu_2O_5$ and Y_2BaCuO_5 is replaced by the Y_2O_3 + L equilibrium. The three-phase fields $Y_2Cu_2O_5$ + Y_2O_3 + L and Y_2BaCuO_5 + Y_2O_3 + L which are formed by reaction p_4 possess a significantly diminished oxygen content compared with the $Y_2Cu_2O_5$ + Y_2BaCuO_5 + L equilibrium which is stable below 1040°C.

4. Conclusions

The ternary eutectic temperature of the Y–Ba–Cu–O system is 899°C at $p(O_2) = 0.21 \times 10^5$ Pa which is much lower than the peritectic decomposition temperature of $YBa_2\ Cu_3O_{7-\delta}$ ($1000 < T < 1020°C$). The corresponding composition is located in the 123–$BaCuO_2$–CuO triangle and possesses a very low $YO_{1.5}$ content (<1.5 mol%). Already at 940°C, Y_2BaCuO_5 forms an equilibrium with the melt which causes a disconnection of the 123–CuO coexistence. Therefore, an overall or local excess of CuO (by inhomogeneities) significantly influences the processing of $YBa_2Cu_3O_{7-\delta}$ above 940°C by local formation of 211 and melt. However, admixtures of 211 do not lead to the appearance of partial melt up to the peritectic decomposition temperature of $YBa_2Cu_3O_{7-\delta}$.

The melting process is always combined with a significant oxygen loss. Therefore, melt and coexisting solid phases do not belong to the same section in view of the oxygen content, and the isothermal sections of Fig. 3 have to be considered as three dimensional projections of a complicated quaternary system. In order to crystallize equilibrium phases from a melt, oxygen diffusion to the crystallization front is a necessary precondition. A kinetic hindrance of the oxygen diffusion or reception considerably affects processing of 123 materials. It also might be the reason for the differences of DTA heating and cooling curves of identical samples. The oxygen partial pressure significantly influences the melting behavior of the considered system.

Acknowledgments

The authors thank Mr. F. Hansch and Mrs. G. Stöver for careful experimental work, Mr. G. Kunze and Mrs. B. Thaut for DTA/TG measurements, and Mrs. C. Heße for XRD analysis, as well as Dr. R. Kucharkowski for chemical analysis. Dr. F. Hohlfeld, TU Dresden, is gratefully acknowledged for placing a computer program to represent quaternary phase diagrams at our disposal. This work is a part of a project granted by the Federal Minister of Science and Technology (BMFT) under No. 13 N 5897.

References

1. G. Krabbes, U. Wiesner, W. Bieger, M. Ritschel, and G. Kunze, *Mater. Sci. Forum* **62–64,** 75 (1990).
2. T. Aselage and K. Keefer, *J. Mater. Res.* **3,** 1279 (1988).
3. T. Aselage, K. D. Keefer, and J. A. Voigt, SAND-89-1514C, Sandia National Laboratories Albuquerque Report, Master Copy (1990).
4. P. Holba, E. Pollert, A. Triska, M. Nevriva, S. Durcok, and L. Matejkova, *in* "Adv. Solid State Chem., Proc. 2nd Intern. Sympos. Solid State Chem., Pardubice, June 26–30, 1989."
5. A. S. Kosmynin, A. A. Fotiev, I. K. Garkushin, G. E. Shter, A. S. Trunin, V. A. Fotiev, and V. A. Balashov, *in* "Fiz.-Khim. Osnovy Sint. i Svoi. VTSP, Anal., Strukt., Svoistva, Akad. Nauk SSSR, Uralsk. Otdel., special issue, Sverdlovsk 1990," p. 39.
6. K. Osamura and W. Zhang, *Z. Metallkd.* **82,** 408 (1991).
7. B.-J. Lee and D. N. Lee, *J. Am. Ceram. Soc.* **72,** 314 (1989).
8. B.-J. Lee and D. N. Lee, *J. Am. Ceram. Soc.* **74,** 78 (1991).
9. N. Nevriva, P. Holba, S. Durcok, D. Zemanova, E. Pollert, and A. Triska, *Physica C* **157,** 334 (1989).
10. R. G. Grebenshchikov, G. A. Mikirticheva, O. G. Zhigareva, and D. P. Romanov, *Dokl. Akad. Nauk SSSR* **302,** 676 (1988).
11. K. W. Lay and G. M. Renlund, *J. Am. Ceram. Soc.* **73,** 1208 (1990).
12. L. McKittrick, L.-Q. Chen, S. Sasayama, M. E. McHenry, G. Kalonji, and R. C. O'Handley, *Adv. Ceram. Mater.* **2,** 353 (1987).
13. G. A. Mikirticheva, V. I. Shitova, O. G. Zhigareva, S. K. Kuchaeva, L. Yu. Grabovenko, and R. G. Grebenshchikov, *Zh. Neorg. Khim.* **35,** 223 (1990).
14. W. Zhang, K. Osamura, and Sh. Ochiai, *J. Am. Ceram. Soc.* **73,** 1958 (1990).
15. G. Krabbes, U. Wiesner, W. Bieger, M. Ritschel, J. Thomas, P. Verges, and Ch. Frenzel, *in* "Proceed. of the 3. German–Soviet Bilateral Seminar on High-Temp. Supercond., Karlsruhe, Oct. 8–12, 1990," special issue, p. 555.
16. J. G. Thompson, J. D. FitzGerald, R. L. Withers, P. J. Barlow, and J. S. Anderson, *Mater. Res. Bull.* **24,** 505 (1989).
17. C. L. Teske and Hk. Müller-Buschbaum, *Z. Naturforsch. B* **27,** 296 (1972).
18. R. S. Roth, K. L. Davis, and J. R. Dennis, *Adv. Ceram. Mater.* **2,** 303 (1987).
19. U. Wiesner, G. Krabbes, and M. Ritschel, *Mater. Res. Bull.* **24,** 1261 (1989).
20. W. Zhang and K. Osamura, *Z. Metallkd.* **81,** 196 (1990).
21. G. M. Kale, *Metal. Trans. A* **23,** 382 (1992); W. Zhang and K. Osamura, *Metal. Trans A* **23,** 382 (1992).
22. L. A. Klinkova, I. V. Sojkina, I. I. Zverkova, S. A. Zverkov, S. A. Shevchenko, and N. I. Ganovich, *in* "Fizikokhim. i Tekhnol. Vysokotemp. Zverchprovod. Mater., Moskva, Sept. 13–15, 1988," p. 41, Nauka (1989).
23. N. Nevriva, E. Pollert, L. Matejkova, and A. Triska, *J. Cryst. Growth* **91,** 434 (1988).
24. G. H. Rao, J. K. Liang, and Z. Y. Qiao, *J. Less-Common Met.* **144,** 215 (1988).
25. L. P. Mesenzeva, V. Ya. Degtyareva, I. A. Bondar, E. V. Bokova, L. A. Doronina, and N. K. Ussakovskaya, *Zh. Neorg. Khim.* **35,** 454 (1990).
26. R. G. Grebenshchikov, G. A. Mikirticheva, O. G. Zhigareva, V. I. Shitova, L. Yu. Grabovenko, and S. K. Kuzhaeva, *in* "Fizikokhim. i Tekhnol. Vysokotemp. Zverchprovod. Mater., Moskva, Sept. 13–15, 1988," p. 33, Nauka (1989).
27. A. A. Fotiev, I. K. Garkushin, C. N. Koshcheeva, F. A. Roshdestvenski, G. E. Shter, V. A. Fotiev, A. S. Kosmynin, and V. D. Shuralev, *in* "Fiz.-Khim. Osnovy Sint. i Svoi. VTSP, Anal., Strukt., Svoistva, Akad. Nauk SSSR, Uralsk. Otdel.," special issue, p. 118 (1990).
28. N. Nevriva, E. Pollert, J. Sestak, L. Matejkova, and A. Triska, *Thermochim. Acta* **136,** 263 (1988).
29. G. Krabbes, W. Bieger, U. Wiesner, and M. Ritschel, *Z. Metallkd.*, submitted.
30. F. Licci, H. J. Scheel, and T. Basagni, *Physica C* **153–155,** 431 (1988).
31. K. Oka, K. Nakane, M. Ito, M. Saito, and H. Unoki, *Jpn. J. Appl. Phys.* **27,** L 1065 (1988).
32. S. Nomura, H. Yoshino, and K. Ando, *J. Cryst. Growth* **92,** 682 (1988).
33. W. Reichelt, H. Wilhelm, G. Försterling, and H. Oppermann, *Cryst. Res. Technol.* **24,** K 26 (1989).
34. F. Licci, P. Tissot, and H. J. Scheel, *J. Less-Common Met.* **150,** 201 (1989).
35. Th. Wolf, W. Goldacker, B. Obst, G. Roth, and R. Flükiger, *J. Cryst. Growth* **96,** 1010 (1989).